

PAPER • OPEN ACCESS

Measurements of the optical and thermal properties of the 2D black phosphorus coating

To cite this article: Paulina Listewnik *et al* 2021 *Mater. Res. Express* **8** 065004

View the [article online](#) for updates and enhancements.



IOP | ebooks™

Bringing together innovative digital publishing with leading authors from the global scientific community.

Start exploring the collection—download the first chapter of every title for free.

Materials Research Express



PAPER

Measurements of the optical and thermal properties of the 2D black phosphorus coating

OPEN ACCESS

RECEIVED

21 April 2021

REVISED

18 May 2021

ACCEPTED FOR PUBLICATION

3 June 2021

PUBLISHED

11 June 2021

Paulina Listewnik* , Małgorzata Szczerska*  and Paweł Jakóbczyk 

Department of Metrology and Optoelectronics, Faculty of Electronics, Telecommunications and Informatics, Gdańsk University of Technology, Narutowicza Street 11/12, 80-233 Gdańsk, Poland

* Authors to whom any correspondence should be addressed.

E-mail: pauliste@student.pg.edu.pl and malszcze@pg.edu.pl

Original content from this work may be used under the terms of the [Creative Commons Attribution 4.0 licence](https://creativecommons.org/licenses/by/4.0/).

Any further distribution of this work must maintain attribution to the author(s) and the title of the work, journal citation and DOI.



Abstract

Black phosphorus is a 2D material, which properties are still being discovered. In this paper, the sensitivity to the temperature of a few-layer black phosphorus coating deposited, on the surface of a microsphere-based fiber-optic sensor, by a dip-coating method is presented. The coating was investigated after 2, 3, and 5 deposition cycles and during temperature growth from 50 °C to 300 °C in an interferometric setup. The intensity of the reflected signal increases with each applied layer. During the investigation of the thermal properties, in the range of 50 °C–200 °C, the polynomial growth rate of the reflected signal can be observed, whereas, for the temperatures over 200 °C, the measured peak intensity of the reflected signal stabilizes at a nearly constant level.

Introduction

From 2010, the year when Andre Geim and Kostya Novoselov were awarded the Nobel Prize in Physics ‘for groundbreaking experiments regarding the two-dimensional material graphene’, there has been intensive work on the development of new 2D materials [1]. From that time on, the group has enriched with many new representatives such as boron nitride (BN) [2], graphitic carbon nitride (g-C₃N₄), metal oxides (e.g. ZnO, TiO₂) [3], metal-organic frameworks (MOFs), molybdenum disulfide (MoS₂) [4], transition metal dichalcogenides (TMDCs) [5] and a single layer of black phosphorus (BP) [6]. On the other hand, the further development of fiber-optic technology - elements as well as entire measurement and imaging systems—is possible only with the use of the latest achievements of material engineering.

Various possibilities of using 2D materials in photonic structures as protective coatings [7], reflective layers, or sensing media were presented [8]. These materials are interesting because of their unique optical properties, as well as geometrical dimensions, which makes the 2D materials the optimal solution for integration with photonic microstructures, e.g., tapers, microrings, microcavities, microdiscs [9–12]. One of the basic problems related to the integration of 2D materials with photonic structures is its effectiveness. So far, thin metal oxides produced by the ALD technique have been used most often in optical fiber technology. Thin carbon-based films were also used by attaching them to optical fiber elements with the use of Van der Waals forces.

The isolation of a thin layer of black phosphorus (in 2013) similarly to graphite by exfoliation using scotch tape began an interest in a new 2D material research field [13]. Phosphorene distinguishes itself from the other two-dimensional materials by a unique puckered honeycomb network and as a result of strong in-plane anisotropy [14]. Thanks to this structure, phosphorene has anisotropic electronic and optical properties. One of the most interesting behaviors of layered black phosphorus is a strong dependence of its properties on layer numbers. For example, a single phosphorene has a bandgap of ca. 2 eV and 0.3 eV in bulk, which provides a wide range of tunability for the band gap [15]. Part of the growing interest in phosphorene can be attributed to the high carrier mobility up to 103 cm²V⁻¹s⁻¹ [16] and moderate on/off ratios 104–105 as well as to the much larger direct bandgap demonstrated in few-layer BP [17]. These properties open a platform to manipulate anisotropic interactions and they enable using phosphorene in electronic and optoelectronic devices as well as sensors, catalysts, capacitors, and batteries [18–22].

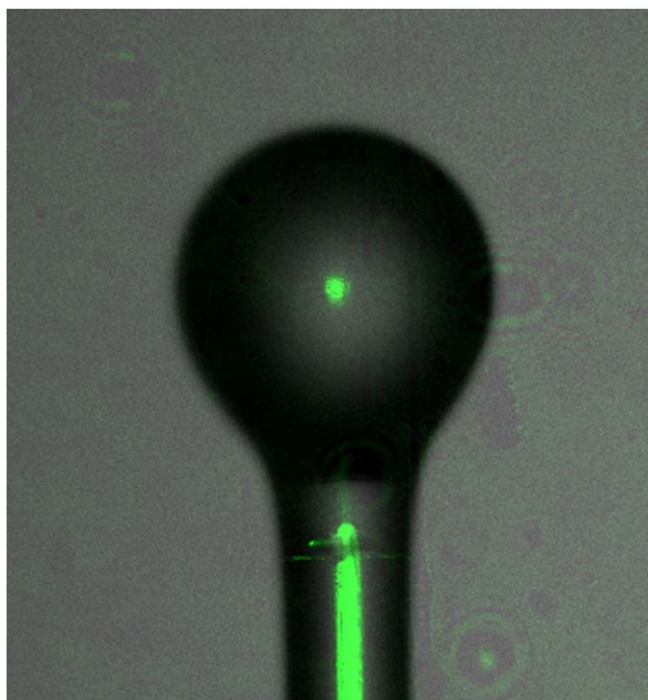


Figure 1. Picture of a microsphere-based fiber-optic sensor fabricated by optical fiber fusion splicer.

In this article, we present the fabrication process of the 2D coating of black phosphorous on the fiber-optic microsphere. The measurements in the low-coherent interferometry set-up allow us to determine how the optical properties of the 2D black phosphorous coating can change while depositing subsequent layers of the material on the surface of a sensor. Furthermore, the thermal properties of the material were investigated in the temperature range from 50 °C to 200 °C.

Materials and methods

The black phosphorus crystals were purchased from Smart Elements. N, N-Dimethylformamide (DMF) was obtained from Sigma Aldrich. All reagents were analytical grade and were used without further purification. The highest purity class argon was collected from Air Liquid.

Few-layer black phosphorus (FLBP) was synthesized via liquid exfoliation from pre-crushed black phosphorus (BP) (30 mg) dispersed in anhydrous, oxygen-free dimethylformamide (7 ml). The process of liquid exfoliation was realized in an ice-cooled bath, in the temperature range of 0 °C–3 °C, under a stream of argon using a horn probe ultrasonicator (Bandelin Sonopuls HD2200, 20 kHz). The sonication tip was set to a power of 40 W with a 0.5/0.5 s ON/OFF time. The exfoliation process took 4 h. Subsequently, the resulting suspension was centrifugated at 11,000 rpm for 45 min to remove the residual unexfoliated particles, yielding blackish-yellow supernatant.

The fiber-optic sensor was manufactured from a standard single-mode telecommunications fiber. To form a microsphere, a fusion splicer (FSU 975, Ericsson Network Technologies AB, Stockholm, Sweden) was used. The splicer incites an electric arc, which causes the fiber to heat up. Simultaneous pulling, at the time, allows obtaining fiber-optic microsphere, due to surface tension occurring at the tip of a fiber. The diameter of the microsphere used for this investigation equals 250 μm. Figure 1. shows a picture of the designed structure obtained by a Stimulated Emission Depletion microscopy (Leica TCS SP8 STED, Germany).

The FLBP was deposited on the surface of a microsphere by the dip-coating technique, in several iterations. Before the beginning of the process, the microstructure was thoroughly cleared of any residual impurities, using isopropanol. Subsequently, the fiber-optic microsphere was immersed in the synthesized supernatant for 1 min, then the sample was left for 24 h to ensure the evaporation of the remaining liquid. The process was repeated five times in an inert environment to prevent oxidation and provide proper deposition of the coating. A schematic of the deposition process is presented in figure 2.

The FLBP coating was characterized by a Raman spectrometer. The Raman spectra were recorded on a micro-Raman spectrometer (InVia, Renishaw, United Kingdom) with a 532 excitation laser (Ar ion laser), and the Raman shift was in the range of 300–600 cm⁻¹ (figure 3).

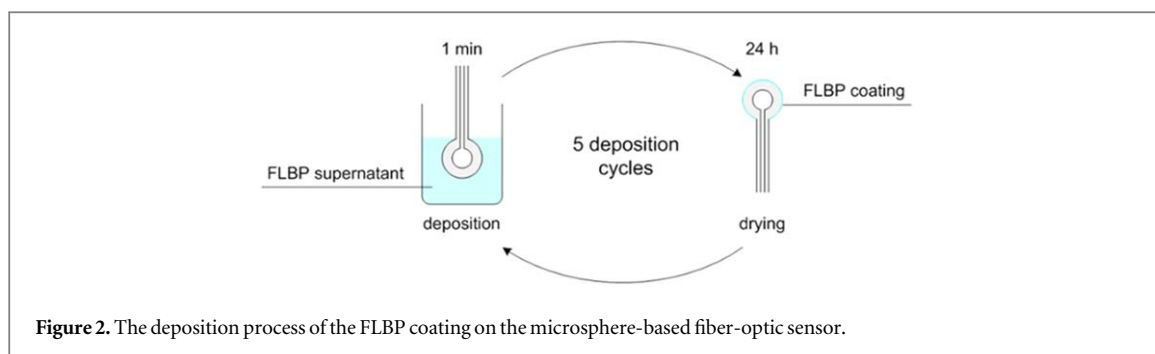


Figure 2. The deposition process of the FLBP coating on the microsphere-based fiber-optic sensor.

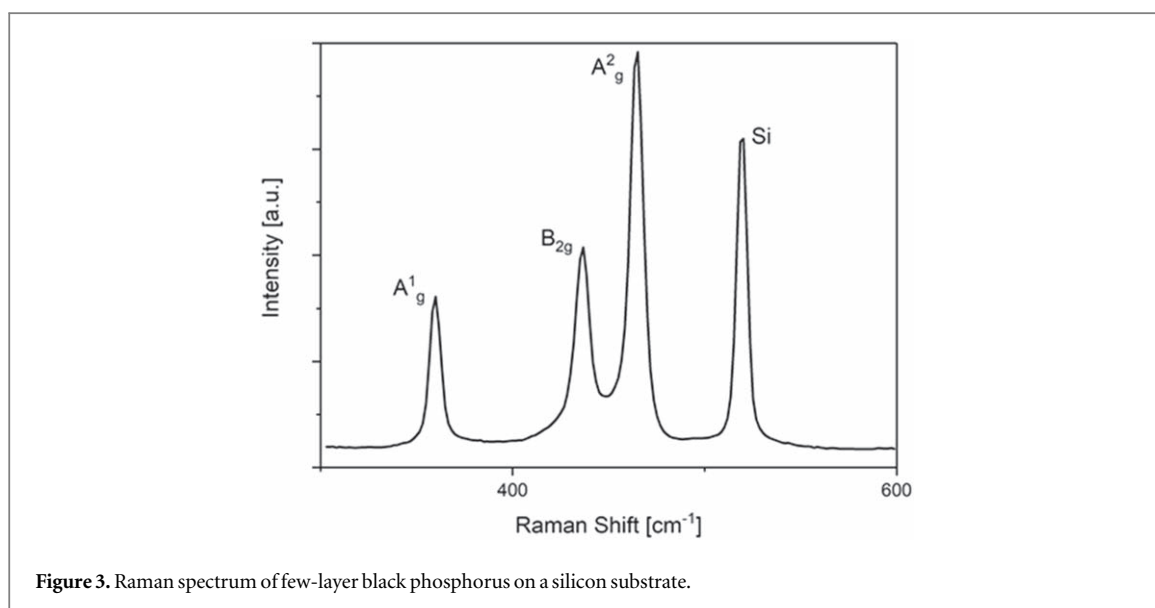


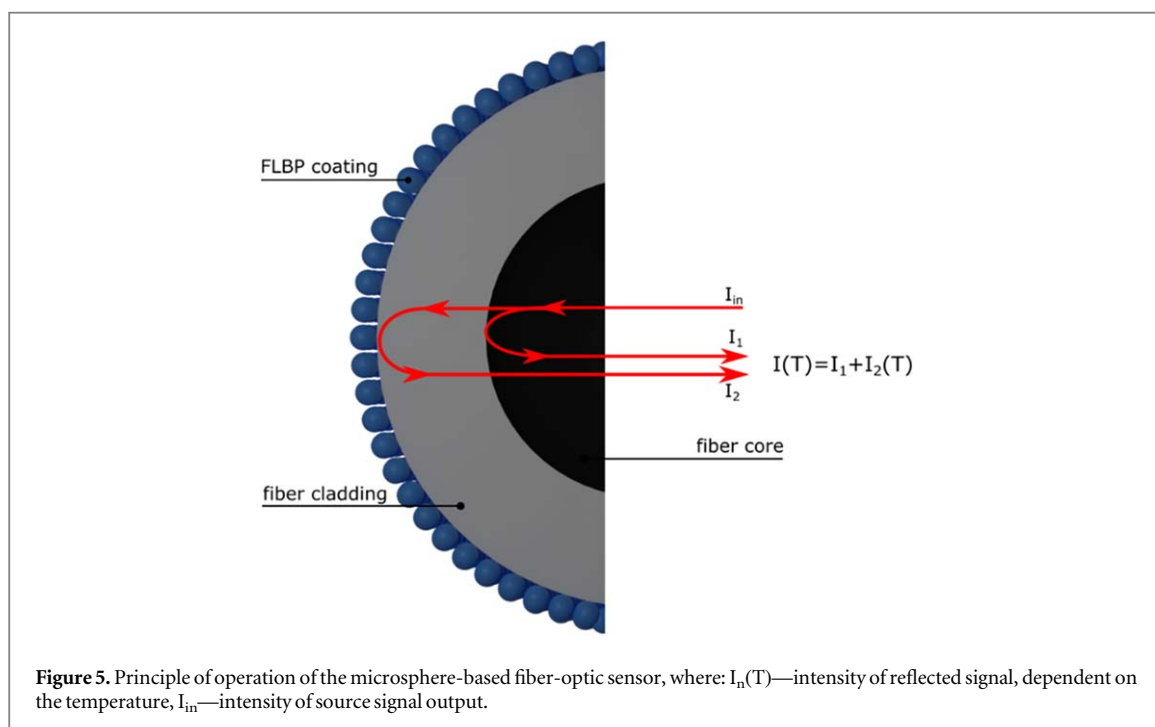
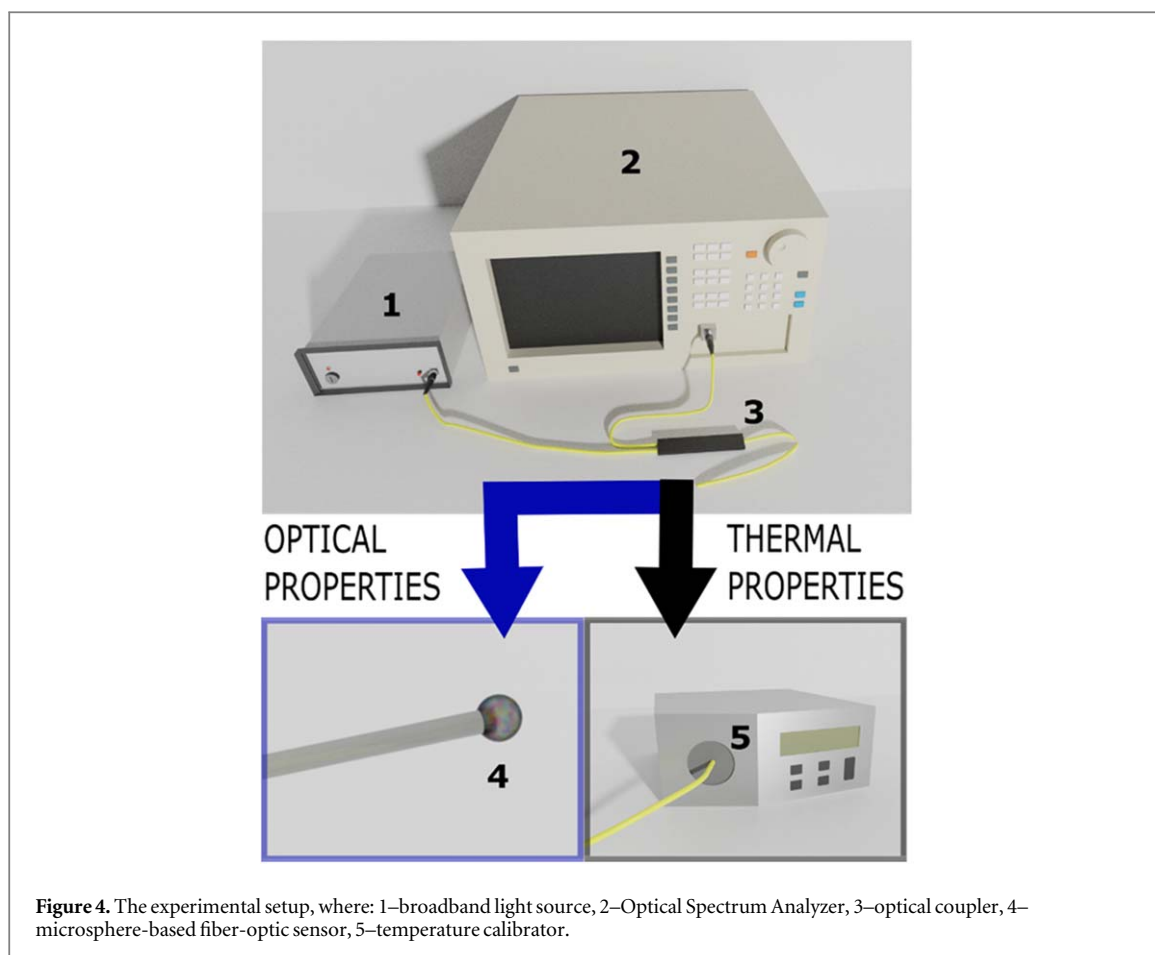
Figure 3. Raman spectrum of few-layer black phosphorus on a silicon substrate.

The phosphorus atoms in phosphorene are covalently linked by sp^3 hybridization and form a quadrangular pyramid structure. Based on the principle of momentum conservation and group theory, Raman spectra should exhibit the six active vibration modes of the 12 lattice vibrational modes [23], but only the three vibration modes A_1^g , A_2^g and B_{2g} are visible when the laser beam is perpendicular to the phosphorene surface [24]. In figure 3, there are three Raman peaks at 359.3 cm^{-1} , 437.0 cm^{-1} , and 464.7 cm^{-1} of a few layer black phosphorus corresponding to the A_1^g , A_2^g and B_{2g} modes, respectively [25]. The peak for the 518.5 cm^{-1} of Raman shift is derived from the silicon substrate. The peak of silicon is clearly visible due to the small and thin phosphorus flakes.

The FLBP coatings of different thicknesses were investigated after the 2nd, 3rd and 5th deposition cycle. The experimental interferometric setup consisted of a light source, fiber-optic devices, an optical analyzer and a sensor head. As the sources, a Compact Laser Diode Driver (CLD1015, Thorlabs Inc., Newton, NJ, USA) with mounted butterfly light source (SLD830S-A20, Thorlabs Inc., Newton, NJ, USA) with a central wavelength of $830 \pm 10 \text{ nm}$, and a light source with a central wavelength of $1310 \pm 20 \text{ nm}$ (SLD-1310-18-W, FiberLabs Inc., Fujimi) were used. The visualization of the experimental setup used during the investigation of the optical and thermal properties of the FLBP coating is shown in figure 4.

The source signal output propagated through the $2 \times 150/50\%$ optical coupler (780 HP, Cellco Communications, Kobylanka, Poland) to the sensor head. A part of the signal was reflected on the boundary created between the core and the cladding of an optical fiber, whereas the rest transmitted through and was reflected on the surface of the sensor, placed directly in the measured medium. Reflected waves superposed, which resulted in interference. An obtained signal was then acquired using Optical Spectrum Analyzer (OSA, Ando AQ6319, Yokohama, Japan) and the data was analyzed.

The principle of operation of a microsphere-based fiber optic sensor is presented in figure 5.



Results and discussion

This section discusses the results obtained for the microsphere-based fiber-optic sensors coated with few-layer black phosphorus (FLBP). Figure 5 shows changes in the intensity of the reflected signal measured before the deposition process and after the deposition of 2, 3, and 5 cycles of FLBP coating. Figure 5(a) shows the spectra of

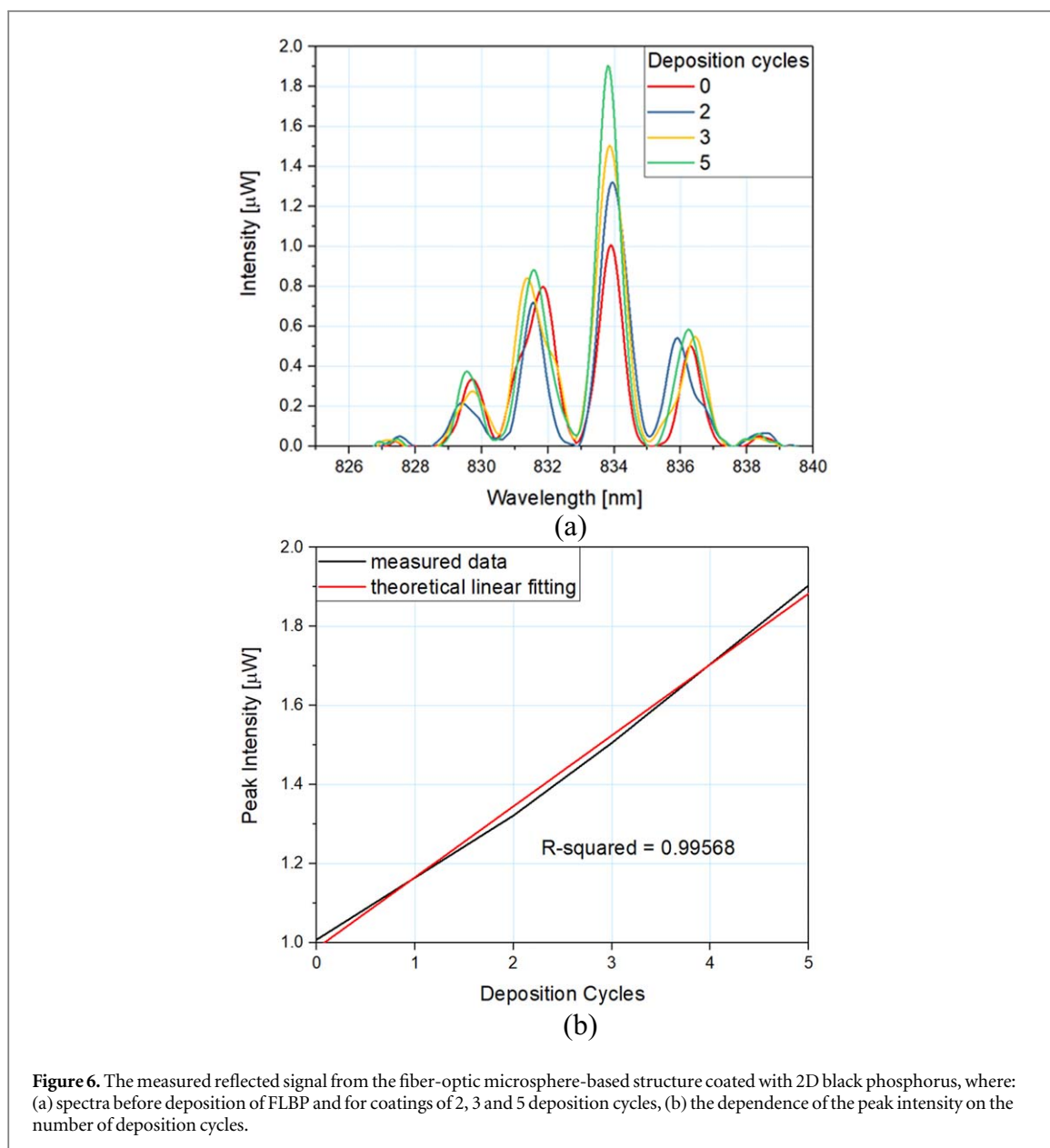
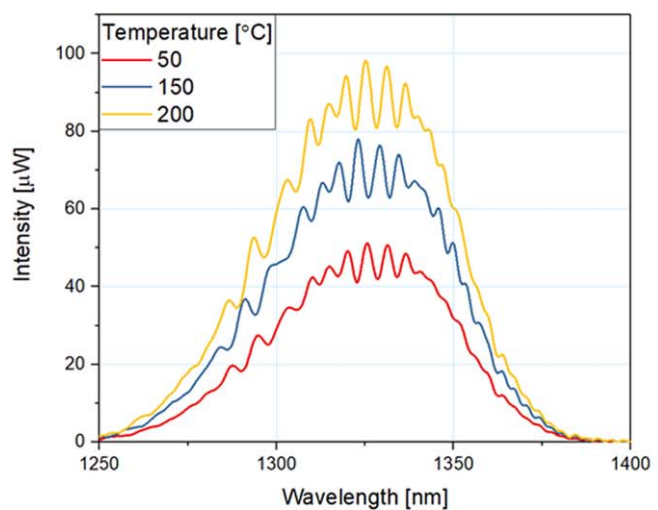


Figure 6. The measured reflected signal from the fiber-optic microsphere-based structure coated with 2D black phosphorus, where: (a) spectra before deposition of FLBP and for coatings of 2, 3 and 5 deposition cycles, (b) the dependence of the peak intensity on the number of deposition cycles.

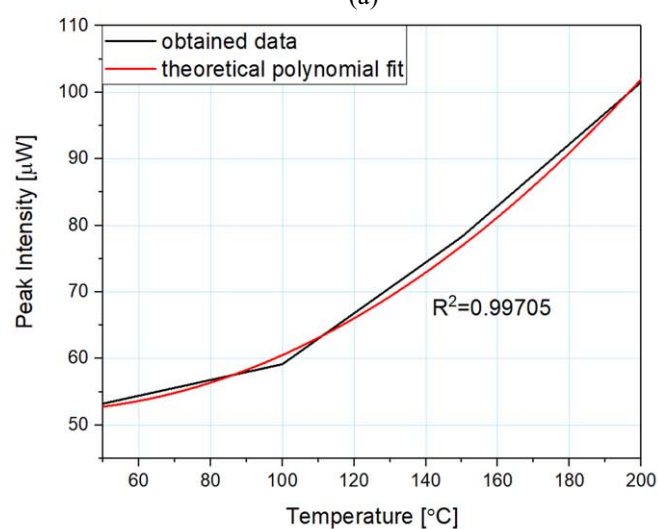
the measured signal for the sensor without a coating and with coatings of 2, 3 and 5 deposition cycles, while in figure 5(b) magnification of the central fringe is presented in order to emphasize the increase of the reflected signal's intensity with a growth of an FLBP coating. The increase in the intensity of the reflected light after successive cycles was caused by a tighter layer forming on the sphere of the optical fiber. The produced FLBP layer acted as a mirror reflecting the light that falls on it. However, the envelope of the spectrum remains similar, after each deposition cycle.

The peak intensity of the reflected signal depends on the number of cycles, in which the coating was deposited, increasing with the increase of the number of coating cycles, as is presented in figure 6(b). It can be observed, the intensity of a reflected signal increases, the thicker the deposited coating. The intensity steadily rises with the number of deposition cycles. Additionally, figure 6(b). Contains a theoretical linear fitting. It proves a close fit to the data obtained from performed measurements. The convergence of the plots is also confirmed by coefficient R^2 , which equals over 0.995.

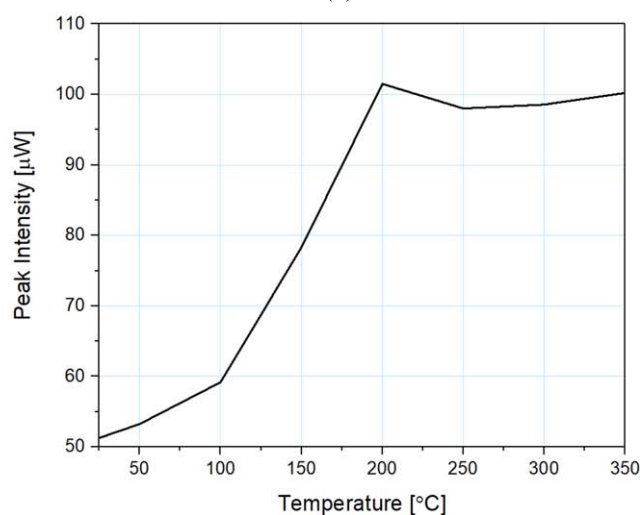
The temperature measurements were performed to evaluate the coating's sensitivity to alternating temperature. The coating was investigated in a range of $50\text{ }^\circ\text{C}$ – $300\text{ }^\circ\text{C}$ with a step of $50\text{ }^\circ\text{C}$. The obtained results are shown in figure 7. Presented measurements contain data registered for the coating of 5 deposition cycles. Figure 7(a) consists of the spectra measured at $50\text{ }^\circ\text{C}$, $100\text{ }^\circ\text{C}$ and $200\text{ }^\circ\text{C}$, figure 7(b) presents the dependence of changing peak intensity of the reflected signal on the altering temperature in the range of $50\text{ }^\circ\text{C}$ – $200\text{ }^\circ\text{C}$, including theoretical polynomial fitting, whereas figure 7(c) shows the measurements in a range $50\text{ }^\circ\text{C}$ – $350\text{ }^\circ\text{C}$.



(a)



(b)



(c)

Figure 7. The measured reflected signal from the fiber-optic microsphere-based sensor during the temperature measurements, where: (a) representative spectra measured at 50, 100, 200 °C for the sensor with a coating of 5 deposition cycles; and reflected signal peak intensity dependence on changing temperature, measured for a coating of 5 deposition cycles, where: (b) range of 50 °C–200 °C with theoretical fitting, (c) range of 50 °C–350 °C.

As shown in figure 7(b), the intensity of the reflected signal increases nearly twice, as the temperature rises. Growth of the reflected signal intensity, depending on temperature setting is closer presented in figures 7(b), (c). The increase in temperature leads to softened atomic bonds and higher phonon velocity, resulting in a higher refractive index and thus in a higher intensity of the reflected signal (figure 7(b)). Such the temperature-dependence of intensity peak proves the FLBP coating is sensitive to the temperature in a range of 50 °C–200 °C. A further increase in temperature above 200 °C does not increase the intensity of the reflected signal peak, which may be related to the anharmonicity of phonons and further the phonon-phonon scattering. A similar dependence on temperature is in the case of thermal conductivity of phosphorene [26, 27]. It can be observed, from polynomial regression, that the obtained data accurately matches the calculated one. Coefficient R^2 equals over 0.997, which proves, the acquired results only slightly vary from the theoretical model.

Conclusion

The successful coating of a few-layer black phosphorous on the surface of the fiber-optic microsphere is reported. This structure was combined with a light source and an optical spectrum analyzer via fiber link to investigate the spectrum of the signal reflected of the black phosphorous layer.

The spectrum of reflected signal from 2, 3 and 5 deposition cycles coating was observed and it was concluded that the reflected signal increases with the increase of the number of layers.

Furthermore, the thermal properties of the few-layer black phosphorous coating in the range of 50 °C to 300 °C was investigated. The increase of the reflected signal from 50 to 200 °C was observed and stabilization of the intensity of the reflected signal at the constant level after 200 °C.

The study has revealed that this is possible to effectively coat the fiber optic structure with few-layers black phosphorus. It can suggest that this 2D material can be used in the fiber optic sensor technology as a reflection layer, which parameters can be tuned by the temperature.

Acknowledgments

Financial support of these studies from Gdańsk University of Technology by the 11/2020/IDUB/I.3/CC grant under the Curium Combating Coronavirus - EIRU program is gratefully acknowledged. The authors acknowledge the financial support DS Programs of the Faculty of Electronics, Telecommunications, and Informatics of the Gdańsk University of Technology and the Polish National Science Centre [2016/22/E/ST7/00102].

Data availability statement

The data that support the findings of this study are available upon reasonable request from the authors.

ORCID iDs

Paulina Listewnik  <https://orcid.org/0000-0002-4857-1019>

Małgorzata Szczerska  <https://orcid.org/0000-0003-4628-6158>

Paweł Jakóbczyk  <https://orcid.org/0000-0002-6528-3713>

References

- [1] Anon 2011 It's still all about graphene *Nature Mater* **10** 1–1
- [2] Gonzalez-Ortiz D, Salameh C, Bechelany M and Miele P 2020 Nanostructured boron nitride-based materials: synthesis and applications *Materials Today Advances* **8** 100107
- [3] Marichy C, Bechelany M and Pinna N 2012 Atomic layer deposition of nanostructured materials for energy and environmental applications *Adv. Mater.* **24** 1017–32
- [4] Li X and Zhu H 2015 Two-dimensional MoS₂: properties, preparation, and applications *Journal of Materiomics* **1** 33–44
- [5] Manzeli S, Ovchinnikov D, Pasquier D, Yazyev O V and Kis A 2017 2D transition metal dichalcogenides *Nat. Rev. Mater* **2** 17033
- [6] Zhang M, Wu Q, Chen H, Zheng Z and Zhang H 2020 Fiber-based all-optical modulation based on two-dimensional materials *2D Mater.* **8** 012003
- [7] Kosowska M, Listewnik P, Majchrowicz D, Rycewicz M, Bechelany M, Flegler Y, Chen M, Fixler D, Dholakia K and Szczerska M 2020 Microscale diamond protection for a ZnO coated fiber optic sensor *Sci. Rep.* **10** 19141
- [8] Hirsch M, Listewnik P, Struk P, Weber M, Bechelany M and Szczerska M 2019 ZnO coated fiber optic microsphere sensor for the enhanced refractive index sensing *Sens. Actuators, A* **298** 111594
- [9] Kou J, Feng J, Ye L, Xu F and Lu Y 2010 Miniaturized fiber taper reflective interferometer for high temperature measurement *Opt. Express* **18** 14245

- [10] Arumona A E, Garhwal A, Youplao P, Amiri I S, Ray K, Punthawanunt S and Yupapin P 2020 Electron cloud spectroscopy using Micro-Ring Fabry–Perot sensor embedded gold grating *IEEE Sensors J.* **20** 10564–71
- [11] Ma J, Ju J, Jin L, Jin W and Wang D 2011 Fiber-tip micro-cavity for temperature and transverse load sensing *Opt. Express* **19** 12418
- [12] Shankar R and Lončar M 2014 Silicon photonic devices for mid-infrared applications *Nanophotonics* **3** 329–41
- [13] Xu Y, Yan B, Zhang H-J, Wang J, Xu G, Tang P, Duan W and Zhang S-C 2013 Large-Gap Quantum Spin Hall Insulators in Tin Films *Phys. Rev. Lett.* **111** 136804
- [14] Eswaraiyah V, Zeng Q, Long Y and Liu Z 2016 Black phosphorus nanosheets: synthesis, characterization and applications *Small* **12** 3480–502
- [15] Tran V, Soklaski R, Liang Y and Yang L 2014 Layer-controlled band gap and anisotropic excitons in few-layer black phosphorus *Phys. Rev. B* **89** 235319
- [16] Xia F, Wang H and Jia Y 2014 Rediscovering black phosphorus as an anisotropic layered material for optoelectronics and electronics *Nat. Commun.* **5** 4458
- [17] Huang Y C, Chen X, Wang C, Peng L, Qian Q and Wang S F 2017 Layer-dependent electronic properties of phosphorene-like materials and phosphorene-based van der Waals heterostructures *Nanoscale* **9** 8616–22
- [18] Irshad R, Tahir K, Li B, Sher Z, Ali J and Nazir S 2018 A revival of 2D materials, phosphorene: Its application as sensors *J. Ind. Eng. Chem.* **64** 60–9
- [19] Jakóbczyk P, Kowalski M, Brodowski M, Dettlaff A, Dec B, Nidzowski D, Ryl J, Ossowski T and Bogdanowicz R 2021 Low-power microwave-induced fabrication of functionalised few-layer black phosphorus electrodes: a novel route towards Haemophilus Influenzae pathogen biosensing devices *Appl. Surf. Sci.* **539** 148286
- [20] Sajedi-Moghaddam A, Mayorga-Martinez C C, Sofer Z, Bouša D, Saievar-Iranizad E and Pumera M 2017 Black phosphorus Nanoflakes/Polyaniline hybrid material for high-performance pseudocapacitors *J. Phys. Chem. C* **121** 20532–8
- [21] Park C-M and Sohn H-J 2007 Black phosphorus and its composite for lithium rechargeable batteries *Adv. Mater.* **19** 2465–8
- [22] Ding K, Wen L, Huang S, Li Y, Zhang Y and Lu Y 2016 Electronic properties of red and black phosphorous and their potential application as photocatalysts *RSC Adv.* **6** 80872–84
- [23] Guo Z et al 2015 From black phosphorus to phosphorene: basic solvent exfoliation, evolution of Raman scattering, and applications to ultrafast photonics *Adv. Funct. Mater.* **25** 6996–7002
- [24] Ribeiro H B, Pimenta M A and de Matos C J S 2018 Raman spectroscopy in black phosphorus *J. Raman Spectrosc.* **49** 76–90
- [25] Dettlaff A, Skowierzak G, Macewicz Ł, Sobaszek M, Karczewski J, Sawczak M, Ryl J, Ossowski T and Bogdanowicz R 2019 Electrochemical stability of few-layered phosphorene flakes on boron-doped diamond: a wide potential range of studies in aqueous solutions *J. Phys. Chem. C* **123** 20233–40
- [26] Qin G and Hu M 2018 Thermal transport in phosphorene *Small* **14** 1702465
- [27] Ong Z-Y, Cai Y, Zhang G and Zhang Y-W 2014 Strong thermal transport anisotropy and strain modulation in single-layer phosphorene *J. Phys. Chem. C* **118** 25272–7